2021 International Conference on Unmanned Aircraft Systems (ICUAS)
Athens, Greece. June 15-18, 2021

Impedance-based Control for Soft UAV Landing on a Ground Robot in Heterogeneous Robotic System

Ivan Kalinov, Alexander Petrovsky, Ruslan Agishev, Pavel Karpyshev, and Dzmitry Tsetserukou

***Abstract*— In this paper, we present a new method for soft landing of an unmanned aerial vehicle (UAV) on a ground robot based on impedance control. It is applied for a heterogeneous robotic system aimed at warehouse stocktaking automation. We describe the operating and mathematical principles of the impedance control for the landing system of the UAV and present the results of the real-world experiments. We evaluate the softness of landing using force sensors attached to each of four legs of the drone by measuring the impact force during the contact. Experimental results revealed that proposed landing impedance control decreased the impact force by 60%. The proposed approach can also be applied for delivery drone landing on the moving truck, cargo ship, or uneven terrain providing low risk of crash accident.**

I. Introduction

A. Motivation

Autonomous robotic systems, especially UAVs, have been gaining popularity in numerous fields of industry, and various tasks from stocktaking in crowded environment [1] and plant disease detection [2] to space monitoring [3] for the decade. The usage of drone technologies itself for solving tasks that industry sets before them, completely changes business models of companies and redraws enterprise landscapes. This trend affects a huge range of industry areas, such as transport, infrastructure, entertainment, insurance, media, agriculture, telecommunication, security, and mining. The sectors that require to solve tasks of high data quality and mobility find drone-based solutions to be most appropriate. One of the most significant advantages of autonomous systems based on UAVs is their vertical takeoff/landing system.

Such systems have to provide the specified accuracy and work autonomously for a long time. One of the most promising tasks for UAVs to automate is warehouse stocktaking. A typical warehouse is a huge building with a large number of racks over 10 meters high with "cells" for pallet-places and pallets inside each cell. Each of them has a unique barcode or, in some cases, RFID marker. In such warehouses all inventory process is done manually. Inventory procedure is as follows: workers put down and scan every pallet manually and after that put it back. It is a very time-consuming and routine procedure which results in a lot of mistakes due to human factor. Full inventory process usually takes three or four days of regular warehouse operation. Automation of this task using a UAV would be an excellent solution, however, there are problems which do not allow to use UAVs for this task: lack of precise localization and navigation systems and short flight time (about 20 minutes). In order to eliminate these disadvantages we have developed a heterogeneous robotic system of two collaborative robots: UAV and unmanned ground robot (UGR) (Fig. 1).

Fig. 1. WareVision: heterogeneous robotic system of UAV and mobile robot aimed at warehouse stocktaking automation.

This system is capable of precise localization and navigation in indoor environment. We developed a robust system for operation in warehouses by dividing localization into two parts for each subsystem, i.e., the UAV and the UGR. The UGR uses a combination of well-known methods for localization and navigation, which is described in the Section II A. Using these methods, the UGR can acquire its global coordinates. The UAV in its turn uses a system of pose estimation relative to the ground robot. This approach allows to acquire the coordinates of the UAV relative to the UGR and then to calculate the global coordinates of the UAV. Also, our solution does not require any infrastructure for the UAV's localization, since all the equipment is installed on the UAV and UGR.

B. Problem statement

For continuous inventory stocktaking in warehouses multiple UAVs can be used along with one UGR, when only one UAV is performing stocktaking at a time while the others are charging. For this approach it is essential to be able to accurately and softly land and take off multiple times in a row. For accurate localization and navigation of the UAV, proper sensor calibration is crucial. However, during a hard landing, such calibration can be lost. Most of the works that investigated the landing of the drone on a mobile platform

All authors are with Space Center of Skolkovo Institute of Science and Technology, Moscow 143026, Russia {ivan.kalinov, aleksandr.petrovskii} @skolkovotech.ru, {ruslan.agishev, pavel.karpyshev, d.tsetserukou} @skoltech.ru

2021 International Conference on Unmanned Aircraft Systems (ICUAS) | 978-1-6654-1535-4/21/$31.00 ©2021 IEEE | DOI: 10.1109/ICUAS51884.2021.9476826

focused on accurate landing, target detection, and landing under various conditions of the system dynamics. In that works, the experiments were carried out either once or each time anew, in other words, the repeatability of the experiments was not investigated. However, soft landing is a critical condition for being able to repeat the experiment. This parameter is fundamental not only for WareVision technology but also for any industrial system based on UAVs. Various methods could be applied for soft landing. For instance, physical softening of the landing surface or/and dampers on the legs. Also, the UAV landing can be softened using software control methods. One of the possible approaches for this task is impedance control which can potentially decrease the impact force while landing.

C. Related works

In the area of scientific problems connected to relative position estimation of unmanned areal vehicles to ground robots, one of the major tasks is landing the UAV on a mobile platform. Precise and reliable UAV landing on non-static objects is a very important and perspective task, since mobile robots working along with UAVs can solve much more problems than a standalone UAV. First of all, in order to land on a mobile platform, a UAV has to work robustly with noisy visual measurements [4]. There are many scientific teams which attempt to achieve precise UAV localization using a camera installed on a UAV detecting and recognising a number of labels on the ground robot, e.g., LEDs (light-emitting diodes), AR (augmented reality) tags, and etc. [5]–[13]. For example, the paper [9] describes the solution utilizing infrared beacons for landing of a fixed-wing UAV. Then, the authors of [14] use a nonlinear controller for a UAV to measure optical flow for the landing control on a moving ground robot. The other studies apply Simultaneous Localization and Mapping (SLAM) algorithms or prediction techniques, e.g., reinforcement learning [15] for landing a UAV in unknown environments. The paper [5] presents an autonomous landing control algorithm for landing a UAV on a mobile platform using Image-based Visual Servoing (IBVS). This algorithm does not allow to track a drone on the altitudes higher than one meter. Falanga et al. [6] developed a drone capable of autonomous landing on a UGR with all on-board sensing and computing systems. Drone recognises a printed marker on the mobile platform. Such solution does not allow to work in environments with poor lighting conditions. Also, the ground robot is not capable of localization and navigation. The authors of [7] proposed a system similar to previous works based on visual tag tracking using the UGR position prediction system. Nevertheless, their approach has the same drawbacks. The authors of [8] presented a design of a landing pad and its relative pose estimation. The paper shows a method where they apply Extended Kalman Filter (EKF) and Extended H∞ (EH∞) to fuse inertial measurement data and the UAV's estimated pose. The authors of this work emphasise that this system can work at maximal altitude of two meters. One of the most promising studies [16] uses a pattern of IR markers for the UAV pose estimation. However, the developed system has low precision of 20 cm on altitude of five meters, which does not allow to use it in warehouse-like environments with narrow aisles between racks.

Impedance control was firstly introduced by Hogan [17]. It is frequently used for human-robot interaction [18], and has found an extended application in haptics [19], teleoperation [20], and rehabilitation [21]. In terms of the application of impedance control for a UAV, several significant papers [22]–[26] have been presented. In [22], authors presented a control architecture that is capable of varying the impedance of the controlled aerial robot and regulating the time-varying interaction forces when contact is detected. The described controller provides a great degree of flexibility to increase performance. They used it only in terms of interacting with a quadrotor during flight. Paper [23] describes a unified framework for external wrench estimation, interaction control and collision detection for flying robots based on impedance control. Authors designed admittance and impedance control, which shapes the robot's disturbance response to external forces. The paper [24] describes the modified impedance control strategy for a generic robotic system that can interact with an unknown environment and a human. The controller makes use of a virtual mass, coupled with the robotic system, which allows for stable interaction. Ruggiero et al. [25] developed a controller ensuring a closed-loop impedance behavior for both the translational and rotational parts of UAV movement. The collision identification technique had been suitably modified and adapted as an estimator of the external generalized forces (forces plus torques) acting on the aerial vehicle. The authors of [26] implemented human-swarm interaction based on impedance-controlled interlinks. Operator guides the swarm of drones by hand movement and feels dynamic state of swarm through tactile patterns at fingertips. The above-mentioned approaches were devoted to the implementation of impedance control for a UAV control during flight and interaction with a human or the environment.

Our main contribution for this work is a new approach for soft landing of UAVs based on an impedance model with landing softness evaluation by measuring the force during the first contact using four force sensors attached to each of four legs.

II. System Overview

In this section we briefly describe the localization and navigation principles of our heterogeneous robotic system and the connection between all key equipment. Our autonomous robotic system consists of the UGR and UAV. The main objective of the UGR is to determine its coordinates relative to the surrounding objects in the warehouse. This allows to accurately calculate the position of each pallet. In order to determine its location in 2D space, the robot uses a SLAM algorithm based on graph-based approaches [27]. For map building of the surveyed area, the robot uses a Light Detection and Ranging device (LIDAR). The robot receives two-dimensional scans and then compares them with local

submaps. Thus, the robot finds its position and complements the map with new obstacles. After that, the UGR combines the submaps into one graph and finds the final terrain map using nonlinear optimization methods. Using a combination of described methods, the UGR localization becomes much more robust, which allows it to operate in a warehouse without external stationary beacons (Fig. 2).

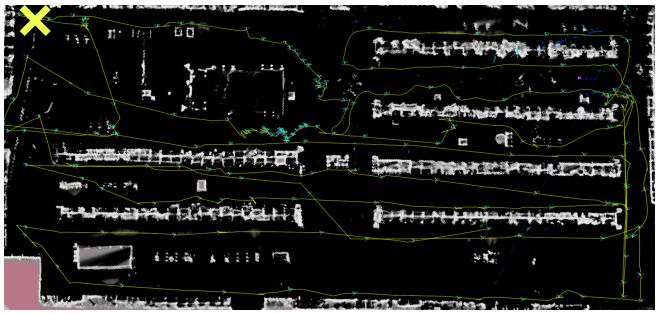

Fig. 2. Localization of the ground robot in a warehouse. The yellow cross indicates the starting point, which coincides with the end point. Colored lines represent the robot's path, white lines indicate obstacles and racks.

For the UAV localization system we use a camera on the ground robot and two concentric patterns of active IR (infrared) markers on the UAV (Fig. 3).

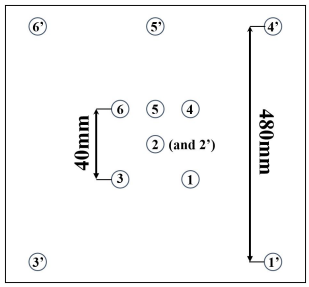

(a) Two concentric patterns.

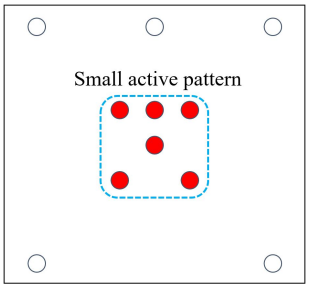

(b) Red circles depict active markers for smaller heights.

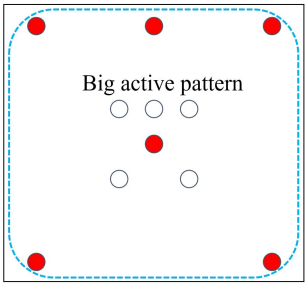

(c) Red circles present active markers for bigger heights.

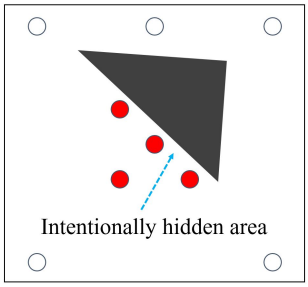

(d) Example of a partially covered pattern that would still be correctly processed.

Fig. 3. IR-patterns used in UAV setup.

The key hardware components and communication links between the UAV and UGR are shown in Fig. 4. As we stated, the goal for the UAV is to fly in a narrow cylindrical working area above the mobile robot. We measure the altitude of the UAV using recognised IR pattern. In our setup, we use an Imaging Source DFK33UX250 2448x2048 camera with a 137.9° field of view (FoV) lens. Also, we have an IR-passing 950 nm filter on the camera to obscure all the light in the visible range and leave only IR-markers in the image.

The detailed explanation of system setup is described in our previous articles [28], [29].

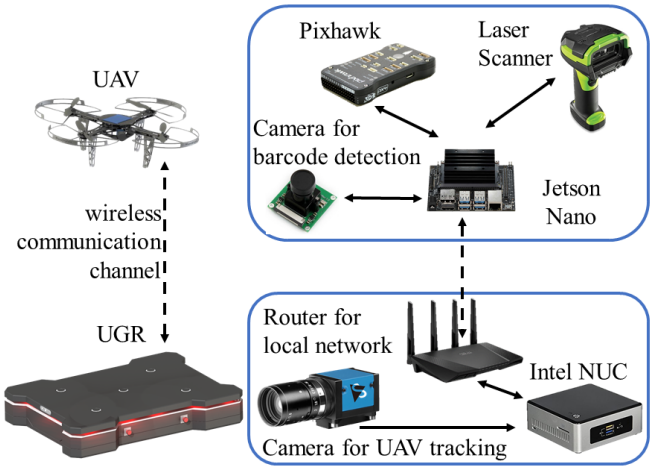

Fig. 4. Communication system setup.

III. Impedance Control for Soft Landing

Our approach for landing the UAV on the UGR is based on the implementation of impedance model where the inputs are position and velocity of the UAV and UGR, and the output is a virtual force that influences the UAV trajectory. In our system the dynamics of the UGR are represented by a system of equations:

$$\begin{cases} \dot{p}_x = v_t \cos\theta \\ \dot{p}_y = v_t \sin\theta \\ \dot{p}_z = 0 \\ \dot{\theta} = a_1 \\ \dot{v}_t = a_2 \end{cases} \tag{1}$$

In Eq. (1), p_x, p_y, p_z are the 3D coordinates of the ground robot position in the world frame, θ is the angle between the X-axis of the robot body frame and the world X-axis, v_t is the tangential velocity of the vehicle, and a_1 and a_2 represent the control input to the system. The dynamic model of the UAV that we use on the altitudes higher than 1 meter is fully described in [23] and is represented by:

$$ma_m = \begin{bmatrix} 0 \\ 0 \\ mg \end{bmatrix} + R_B^N \begin{bmatrix} 0 \\ 0 \\ -\chi \end{bmatrix} + F_D, \tag{2}$$

where m is the mass of the UAV, a_m is the total acceleration of the UAV, g is the nominal acceleration, χ is the total thrust generated by the UAV rotors, F_D is the air drag force, and R_B^N is the rotation matrix from the NED reference frame to the body frame:

$$R_B^N = \begin{bmatrix} c_\theta c_\psi & s_\phi s_\theta c_\psi - c_\phi s_\psi & c_\phi s_\theta c_\psi + s_\phi s_\psi \\ c_\theta s_\psi & s_\phi s_\theta s_\psi + c_\phi c_\psi & c_\phi s_\theta s_\psi - s_\phi c_\psi \\ s_\theta & s_\phi c_\theta & c_\phi c_\theta \end{bmatrix} \tag{3}$$

The force equations can be simplified in the following way:

$$m \begin{bmatrix} \ddot{x}_m \\ \ddot{y}_m \\ \ddot{z}_m \end{bmatrix} = \begin{bmatrix} 0 \\ 0 \\ mg \end{bmatrix} - \begin{bmatrix} c_\phi s_\theta c_{\psi z} + s_\phi s_\psi \\ c_\phi s_\theta s_\psi - s_\phi c_\psi \\ c_\phi c_\theta \end{bmatrix} \chi - \begin{bmatrix} k_d \dot{x}_m |\dot{x}_m| \\ k_d \dot{y}_m |\dot{y}_m| \\ k_d \dot{z}_m |\dot{z}_m| \end{bmatrix} \tag{4}$$

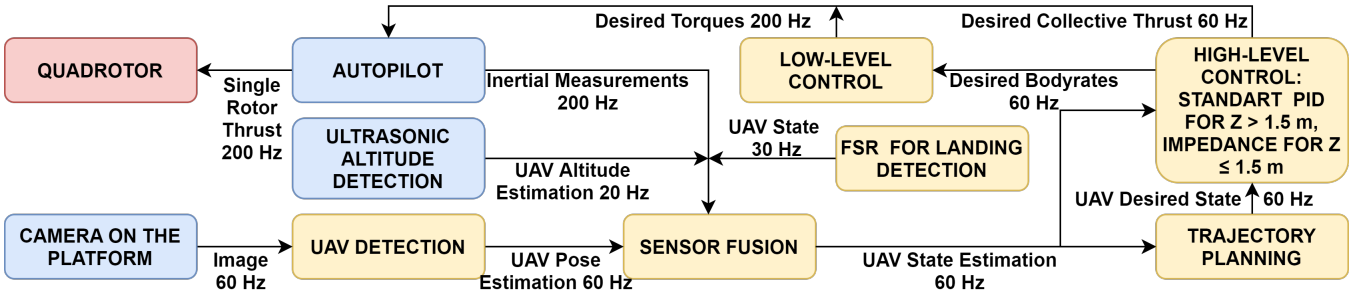

Fig. 5. The schematic of the system framework.

During the landing from altitudes less than 1.5 meters we add a virtual force that does not allow the quadrotor to land quickly and be damaged in the moment of landing. Fig. 5 presents our framework where yellow, blue, red blocks represent software modules, hardware components, and quadrotor, respectively. Communication between modules is done in Robot Operating System (ROS). Implementation of the virtual force changes the dynamic model of the UAV to:

$$m\begin{bmatrix}\ddot{x}_m\\ \ddot{y}_m\\ \ddot{z}_m\end{bmatrix}=\begin{bmatrix}0\\0\\mg\end{bmatrix}-\begin{bmatrix}c_\phi s_\theta c_\psi+s_\phi s_\psi\\ c_\phi s_\theta s_\psi-s_\phi c_\psi\\ c_\phi c_\theta\end{bmatrix}\chi+F_D-F_{imp}, \tag{5}$$

where F_{imp} is the virtual impedance force applied to the UAV. In order to calculate the correction for the UAV goal position, we need to solve the second order differential equation for each coordinate:

$$\begin{bmatrix}M_d^x\ddot{x}_{imp}\\ M_d^y\ddot{y}_{imp}\\ M_d^z\ddot{z}_{imp}\end{bmatrix}+\begin{bmatrix}D_d^x\dot{x}_{imp}\\ D_d^y\dot{y}_{imp}\\ D_d^z\dot{z}_{imp}\end{bmatrix}+\begin{bmatrix}K_d^x x_{imp}\\ K_d^y y_{imp}\\ K_d^z z_{imp}\end{bmatrix}=\begin{bmatrix}F_{imp}^x(t)\\ F_{imp}^y(t)\\ F_{imp}^z(t)\end{bmatrix} \tag{6}$$

where $\Delta x_{imp}=x_{imp}^c-x_{imp}^d$ is the difference between current and desired position, M_d is the desired mass of the virtual UAV body, D_d is the desired damping coefficient, and K_{dis} is the desired stiffness. In our experiments we use this model only in application to the Z-axis in term of our ground robot being static (Fig. 6). Based on this evidence, we could write the impedance equation for Z-axis in discrete time-space domain:

$$\begin{bmatrix}\Delta z_{k+1}\\ \Delta\dot{z}_{k+1}\end{bmatrix}=A_d\begin{bmatrix}\Delta z_k\\ \Delta\dot{z}_k\end{bmatrix}+B_dF_{imp}^k, \tag{7}$$

where $A_d=e^{AT}$,$B_d=(e^{AT}-I)A^{-1}B$, T is the sampling time, I is the identity matrix, and e^{AT} is the state transition matrix. In our system A and B are equal to:

$$A=\begin{bmatrix}0 & 1\\ -\frac{K_d^z}{M_d^z} & -\frac{D_d^z}{M_d^z}\end{bmatrix} \tag{8}$$

$$B=\begin{bmatrix}0\\ -1/M_d^z\end{bmatrix} \tag{9}$$

We can find A_d and B_d from Cayley-Hamilton theorem. For the case of overdamped second order system we have the following solution:

$$A_d=e^{\lambda T}\begin{bmatrix}1-\lambda T & T\\ -\frac{K_d^z}{M_d^z}T & 1-\lambda T+\frac{D_d^z}{M_d^z}T\end{bmatrix} \tag{10}$$

$$B_d=\frac{1}{K_d^z}\begin{bmatrix}e^{\lambda T}(1-\lambda T)-1\\ -\frac{K_d^z}{M_d^z}Te^{\lambda T}\end{bmatrix}, \tag{11}$$

where λ is the eigenvalue variable of the matrix A.

Then, we use A_d and B_d to calculate the impedance correction term x_{imp}^c for the current position of the UAV. In order to control the UAV during landing by $F_{imp}^z(t)$, the force must be formalized using the UAV state parameters e.g., speed and acceleration. As landing softness depends on the UAV speed we propose to calculate the impedance force as the function of the UAV velocity along Z-axis:

$$F_{imp}^z(t)=-k_v^z\dot{z}(t), \tag{12}$$

where k_v^z is the scaling coefficient.

In terms of landing of the UAV on the moving mobile platform the impedance force along X and Y axes could be a function of the platform velocities $\dot{p}_x$ and $\dot{p}_y$:

$$F_{imp}^x(t)=-k_v^x\dot{p}_x(t) \tag{13}$$

$$F_{imp}^y(t)=-k_v^y\dot{p}_y(t) \tag{14}$$

To evaluate the performance of the proposed impedance-based UAV landing algorithm, the experiments needs to be conducted.

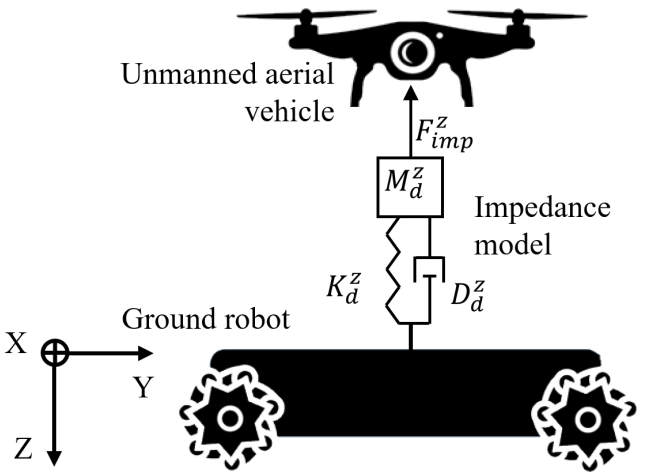

Fig. 6. Impedance model during the UAV landing.

IV. Landing Experiments

It is well known that the behavior of an impedance model described with the second-order ordinary differential equation of the type 6, in general, is divided into several modes, based on the choice of M_d^z, D_d^z, K_d^z coefficients: undamped, underdamped, critically damped, overdamped.

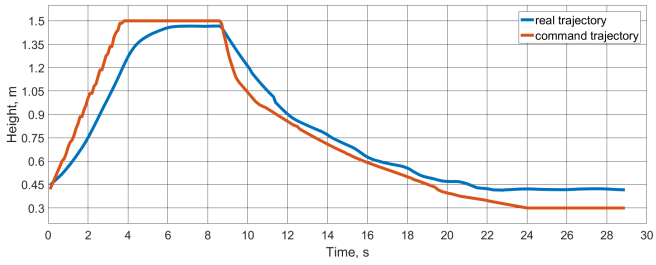

(a) Trajectory of the UAV along Z axis.

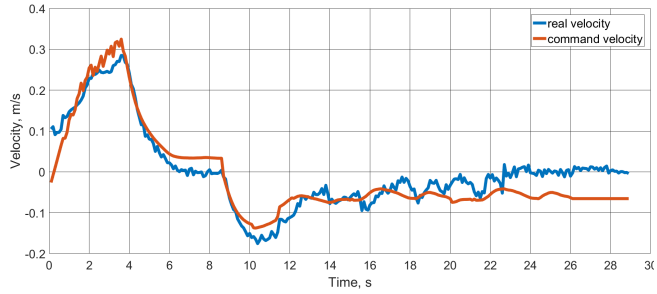

(b) Velocity of the UAV along Z axis.

Fig. 7. Impedance control method during the UAV landing.

The main goal of the proposed impedance control-based model is to make the drone's landing trajectory smooth and decrease the UAV's velocity. Because of this fact, the critically damped and overdamped model is more preferable. In our case, the coefficients were selected as follows: $M_d^z = 1.0\ [kg]$, $D_d^z = 37.8\ [Ns/m]$, $K_d^z = 2.0\ [N/m]$, in order to provide the overdamped response which would decelerate the UAV slowly enough in order to touch the ground robot with the velocity close to zero. For better understanding, we flipped the Z axis in Fig. 7-8, despite the fact that in the Section III it is pointing down, as shown in Fig. 6. We present the landing trajectory with impedance control method in Fig. 7a. The drone adapts its velocity during landing starting at second 9 (see Fig. 7b). The UAV starts its descending with a maximum velocity $V_z = 0.18\ [m/s]$ and then decelerates gradually until reaching a small constant speed, $V_z = 0.05\ [m/s]$ at second 20, at which it afterwards reaches the UGR (the height of the UGR is of 40 cm).

During the first experiments, we noted that the UAV almost reached the UGR already at the 22^{nd} sec of flight. Despite this fact, the final landing was not carried out for about 7 seconds. Because of this, the UAV began to drift from side to side due to aerodynamic effects. In addition, such drift is extremely undesirable for the operation of the UAV localization system, since the field of view of the camera at such low altitudes is extremely small and at any moment the position of the UAV may be lost. The main task of the presented robotic heterogeneous system is to carry out

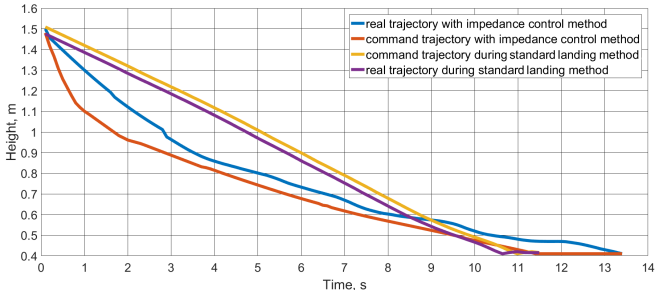

Fig. 8. Trajectories along Z axis during the UAV landing.

inventory autonomously at warehouses; it is essential for us to land not only softly but also accurately. The force sensors on each leg of the UAV were used for landing detection. Therefore, we tested the following landing algorithm: at the height of 1.5 meters the impedance landing model turns on and works until one of the force sensors detects the first contact with the UGR, after that the rotors turn off and the UAV lands, we called this method "Landing detection". Proposed approach allows us to reduce the UAV speed in comparison with the standard landing method and also reduce the duration of landing in comparison with the first impedance approach, that we called "No landing detection". Fig. 8 represents real and command trajectories during standard landing method of the Pixhawk flight controller and during proposed impedance-based control method. Using this approach we reduced the landing time from 20.4 sec to 13.3 sec in comparison with 11.4 sec in the standard method.

The force sensors attached to each leg were also used to evaluate the softness of landing by measuring the mean force during the first contact as the most reliable parameter of softness. We apply Force Sensitive Resistors (FSR 402). The data is collected using Arduino Uno recording analog input 30 times per second. For each method, we produce up to 15 attempts of landing to compare them according to 8 parameters: maximal and mean velocities (V_{max}, $\overline{V}$), maximal and mean accelerations (a_{max}, $\overline{a}$), maximal and mean forces during the first contact (F_{max}, $\overline{F}$), maximal and mean duration of landing (t_{max}, $\overline{t}$), respectively. The results of the comparison are presented in Table I.

TABLE I
Comparison of Two Methods

	Standard method	Impedance-based methods	
		No landing detection	Landing detection
$\overline{a}, m/s^2$	4,93	4,49	**4,45**
$\overline{V}, m/s$	0,14	**0,06**	0,11
$\overline{t}, s$	**11,1**	19,8	**13,1**
$\overline{F}, N$	6,7	**2,55**	**2,7**
$a_{max}, m/s^2$	5,41	5,33	**5,29**
$V_{max}, m/s$	**0,23**	0,24	0,24
t_{max}, s	**11,8**	21,1	**14,2**
F_{max}, N	7,3	**3,1**	**2,9**

Fig. 9 shows the box-plot for forces at the moment of the first contact of the UAV with UGR for all methods. To evaluate the result and find the most optimal method we introduce the coefficient of optimal landing (the lower value of the coefficient means more optimal landing):

$$C_{landing} \sim \overline{F}\overline{t} \tag{15}$$

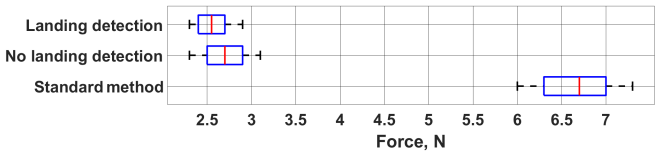

Fig. 9. Box-plot of forces at the first moment upon landing of the UAV

This coefficient could be modified by using a weight component for force and landing duration. In our case, we estimate the weight component equals to 1.0. In accordance with this fact, the most optimal was the impedance-based method with landing detection.

V. Conclusions

We have developed operating and mathematical principles of the impedance control for the landing system of the UAV and presented the results of real-world experiments. This approach has been developed to support continuous operation of the heterogeneous robotic system during automated warehouse stocktaking. We evaluated the softness of landing using the force sensors attached to each drone leg using measurements of the force during the first contact. Our experiments showed that the developed method of adaptive landing allows to reduce the force during the first contact in 2.5 times. Based on this evidence we conclude that the proposed impedance control for a UAV landing will considerably decrease the risk of damaging a drone and onboard equipment. Further work will be devoted to conducting the experiments of the landing of the UAV on the moving robot with adaptive impedance control.

Acknowledgment

The reported study was funded by RFBR and CNRS, project number 21-58-15006.

References

[1] A. Petrovsky, I. Kalinov, P. Karpyshev, M. Kurenkov, V. Ramzhaev, V. Ilin, and D. Tsetserukou, "Customer behavior analytics using an autonomous robotics-based system," in *2020 16th International Conference on Control, Automation, Robotics and Vision (ICARCV)*, pp. 327–332, IEEE, 2020.

[2] P. Karpyshev, V. Ilin, I. Kalinov, A. Petrovsky, and D. Tsetserukou, "Autonomous mobile robot for apple plant disease detection based on cnn and multi-spectral vision system," in *2021 IEEE/SICE International Symposium on System Integration (SII)*, pp. 157–162, IEEE, 2021.

[3] D. Yatskin and I. Kalinov, "Principles of solving the space monitoring problem by multirotors swarm," in *2017 IVth International Conference on Engineering and Telecommunication (EnT)*, pp. 47–50, IEEE, 2017.

[4] I. Kalinov and R. Agishev, "Effective detection of real trajectories of highly maneuverable uavs under strong noise conditions," in *2018 Engineering and Telecommunication (EnT-MIPT)*, pp. 193–196, IEEE, 2018.

[5] D. Lee, T. Ryan, and H. J. Kim, "Autonomous landing of a vtol uav on a moving platform using image-based visual servoing," in *2012 IEEE International conference on robotics and automation*, pp. 971–976.

[6] D. Falanga, A. Zanchettin, A. Simovic, J. Delmerico, and D. Scaramuzza, "Vision-based autonomous quadrotor landing on a moving platform," in *2017 IEEE International Symposium on Safety, Security and Rescue Robotics (SSRR)*, pp. 200–207, IEEE, 2017.

[7] A. Rodriguez-Ramos, C. Sampedro, H. Bavle, Z. Milosevic, A. Garcia-Vaquero, and P. Campoy, "Towards fully autonomous landing on moving platforms for rotary unmanned aerial vehicles," in *2017 International Conference on Unmanned Aircraft Systems (ICUAS)*, pp. 170–178, IEEE, 2017.

[8] O. Araar, N. Aouf, and I. Vitanov, "Vision based autonomous landing of multirotor uav on moving platform," *Journal of Intelligent & Robotic Systems*, vol. 85, no. 2, pp. 369–384, 2017.

[9] V. Khithov, A. Petrov, I. Tishchenko, and K. Yakovlev, "Toward autonomous uav landing based on infrared beacons and particle filtering," in *Robot Intelligence Technology and Applications 4*, pp. 529–537, Springer, 2017.

[10] C. S. Sharp, O. Shakernia, and S. S. Sastry, "A vision system for landing an unmanned aerial vehicle," in *Proceedings 2001 ICRA. IEEE International Conference on Robotics and Automation (Cat. No. 01CH37164)*, vol. 2, pp. 1720–1727, Ieee, 2001.

[11] P. Serra, R. Cunha, T. Hamel, D. Cabecinhas, and C. Silvestre, "Landing of a quadrotor on a moving target using dynamic image-based visual servo control," *IEEE Transactions on Robotics*, vol. 32, no. 6, pp. 1524–1535, 2016.

[12] K. E. Wenzel, A. Masselli, and A. Zell, "Automatic take off, tracking and landing of a miniature uav on a moving carrier vehicle," *Journal of intelligent & robotic systems*, vol. 61, no. 1-4, pp. 221–238, 2011.

[13] Y. Bi and H. Duan, "Implementation of autonomous visual tracking and landing for a low-cost quadrotor," *Optik-International Journal for Light and Electron Optics*, vol. 124, no. 18, pp. 3296–3300, 2013.

[14] B. Herissé, T. Hamel, R. Mahony, and F.-X. Russotto, "Landing a vtol unmanned aerial vehicle on a moving platform using optical flow," *IEEE Transactions on robotics*, vol. 28, no. 1, pp. 77–89, 2011.

[15] R. Polvara, M. Patacchiola, S. Sharma, J. Wan, A. Manning, R. Sutton, and A. Cangelosi, "Autonomous quadrotor landing using deep reinforcement learning," *arXiv preprint arXiv:1709.03339*, 2017.

[16] M. Faessler, E. Mueggler, K. Schwabe, and D. Scaramuzza, "A monocular pose estimation system based on infrared leds," in *International Conference on Robotics and Automation (ICRA)*, pp. 1–6, IEEE, 2014.

[17] N. Hogan, "Impedance control: An approach to manipulation," in *1984 American control conference*, pp. 304–313, IEEE, 1984.

[18] D. Tsetserukou, R. Tadakuma, H. Kajimoto, and S. Tachi, "Optical torque sensors for implementation of local impedance control of the arm of humanoid robot," in *Proceedings IEEE International Conference on Robotics and Automation (ICRA)*, pp. 1674–1679, IEEE, 2006.

[19] R. J. Adams and B. Hannaford, "Stable haptic interaction with virtual environments," *IEEE Transactions on robotics and Automation*, vol. 15, no. 3, pp. 465–474, 1999.

[20] L. J. Love and W. J. Book, "Force reflecting teleoperation with adaptive impedance control," *IEEE Transactions on Systems, Man, and Cybernetics, Part B*, vol. 34, no. 1, pp. 159–165, 2004.

[21] S. Hussain, S. Q. Xie, and P. K. Jamwal, "Adaptive impedance control of a robotic orthosis for gait rehabilitation," *IEEE transactions on cybernetics*, vol. 43, no. 3, pp. 1025–1034, 2013.

[22] A. Y. Mersha, S. Stramigioli, and R. Carloni, "Variable impedance control for aerial interaction," in *2014 IEEE/RSJ International Conference on Intelligent Robots and Systems*, pp. 3435–3440, IEEE, 2014.

[23] T. Tomić and S. Haddadin, "A unified framework for external wrench estimation, interaction control and collision reflexes for flying robots," in *2014 IEEE/RSJ International Conference on Intelligent Robots and Systems*, pp. 4197–4204, IEEE, 2014.

[24] M. Fumagalli and R. Carloni, "A modified impedance control for physical interaction of uavs," in *2013 IEEE/RSJ International Conference on Intelligent Robots and Systems*, pp. 1979–1984, IEEE, 2013.

[25] F. Ruggiero, J. Cacace, H. Sadeghian, and V. Lippiello, "Impedance control of vtol uavs with a momentum-based external generalized forces estimator," in *2014 IEEE International Conference on Robotics and Automation (ICRA)*, pp. 2093–2099, IEEE, 2014.

[26] E. Tsykunov, L. Labazanova, A. Tleugazy, and D. Tsetserukou, "Swarmtouch: tactile interaction of human with impedance controlled swarm of nano-quadrotors," in *IEEE/RSJ International Conference on Intelligent Robots and Systems (IROS)*, pp. 4204–4209, IEEE, 2018.

[27] W. Hess, D. Kohler, H. Rapp, and D. Andor, "Real-time loop closure in 2D LIDAR SLAM," in *2016 IEEE International Conference on Robotics and Automation (ICRA)*, pp. 1271–1278, IEEE, may 2016.

[28] I. Kalinov, E. Safronov, R. Agishev, M. Kurenkov, and D. Tsetserukou, "High-precision uav localization system for landing on a mobile collaborative robot based on an ir marker pattern recognition," in *2019 IEEE 89th Vehicular Technology Conference*, pp. 1–6, IEEE, 2019.

[29] I. Kalinov, A. Petrovsky, V. Ilin, E. Pristanskiy, M. Kurenkov, V. Ramzhaev, I. Idrisov, and D. Tsetserukou, "Warevision: Cnn barcode detection-based uav trajectory optimization for autonomous warehouse stocktaking," *IEEE Robotics and Automation Letters*, vol. 5, no. 4, pp. 6647–6653, 2020.